

Figure 26: Blue: The electrons with the highest kinetic energy around t_0 (integrated over 100 meV). They are found at a kinetic energy of 3.85 eV and red: the Gaussian fit to model the position of time zero. Fitting parameters can be found in the text.

To model the Gaussian shape of the electron distribution the full width at half maximum (FWHM) of the Gaussian was held at the measured cross-correlation of 84 fs, assuming no broadening by propagation. The offset to account for the background, the amplitude and time offset was varied. The time offset was set to 0 after the variation is done. The Gaussian fit is used, because the probe beam convolves with the electron distribution generated by the pump beam generating a cross-correlation, that is broadened by the Gaussian shape of the pulses. Then E_F needs to be defined as zero to be a reference between the different measurements. Because all measurements with different sample positions had different count rates, an energy below E_F is chosen, where all measurements are normalised to 1.

4 Analysis



4.1 Calculation of Laser Absorption Profile



For the calculation of the laser absorption profile the program X-op was used [43, 16]. Details on the analysis can be found in Sec. 2.3. The program was originally designed to simulate X-ray diffraction in crystals, but it can likewise be used for our laser profiles by amending the necessary data sets. To calculate the absorption depth of the 800 nm and 200 nm light beams the program needs several optical constants, which were taken from Weaver[41] for Au and Palik[33] for Fe and MgO. The procedure

from Eschenlohr et al. was used, who simulated a similar heterostructural system of Au/ Ni/ Pt/ Al [18]. The following systems were calculated, see table 2.

Table 2: X-op inputs FP means front side pump, BP means back side pump

Au thickness [nm]	Fe thickness [nm]	laser geometry
5	7	FP and BP
15	7	FP and BP
30	7	FP and BP

The angle of incident for the calculations is 45° and the light polarisation was parallel, like the experiments performed. All BP-geometries were simulated with and without the MgO-substrate by changing the environment from vacuum to MgO, but it did not affect the results.

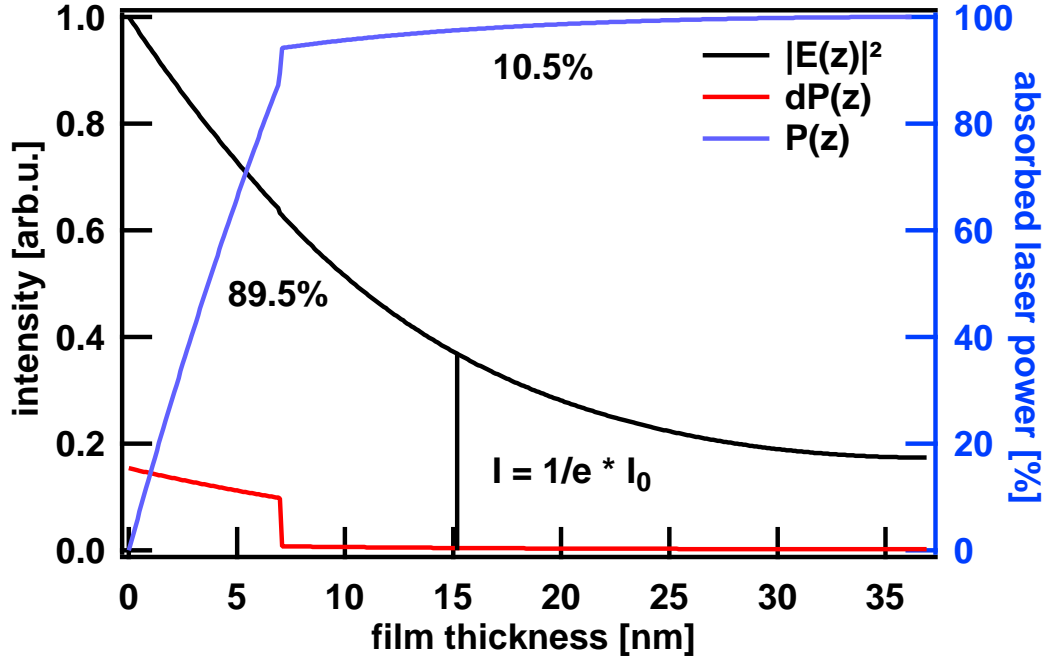


Figure 27: Laser absorption profile for the 800 nm on the back side of 30 nm Au / 7 nm Fe. With the black trace as the intensity of the electric field of the light, the blue the absorbed laser power $P(z)$ normalised to one at the end of the sample and the red trace showing the differential of the absorbed laser power $dP(z)/dz$. The first 7 nm are the Fe film.

Fig. 27 shows the square of the absolute value of the electric field (black line), the absorbed laser power (blue line) and the change in the absorbed laser power dP/dz (red line), plotted against the position in the heterostructure along the surface normal for 30 nm Au in BP geometry. The first 7 nm are the Fe film. For the square of the absolute value of the electric field one can observe an exponential decrease in field

intensity with a slight kink right at the Au/Fe-interface. This kink is due to the numerical solution of the X-ray calculations and the convergence at the interface. The absorbed laser power $P(z)$ was normalised to 1 at the end of the calculated sample to get an idea of the proportions of absorption in the heterostructure system. The optical penetration depth λ_{OPD} of the laser beams, was estimated to the transmitted intensity dropping to $1/e$ of the incident value



$$I_{transmitted} = \frac{1}{e} = \lambda_{OPD} \quad (11)$$

This gave different optical penetration depths for the different systems, due to changing optical parameters of Fe and Au, but similarly due to the various internal reflections in different sample thicknesses. For the 800 nm beam the λ_{OPD} is shown in the following table 3

Table 3: Estimated λ_{OPD} in nm for the 1.55 eV beam. ~~FP meaning frontside pump and BP back side pump.~~

laser geometry	5 nm Au	15 nm Au	30 nm Au
FP	N/A	N/A	14.8
BP	N/A	N/A	15.3



Only for the 30 nm Au samples enough of the laser intensity gets absorbed and reflected so that this work can estimate an λ_{OPD} for the 1.55 eV pump beam. This means that we are homogeneously exciting the sample in the laser spot without creating a diffusion gradient away from the excited surface. If we look at the calculations for the 6 eV probe beam, see Fig. 28, we observe much more absorption in Au even for 5 nm film thickness, when compared to the 1.55 eV in front side pump configuration.

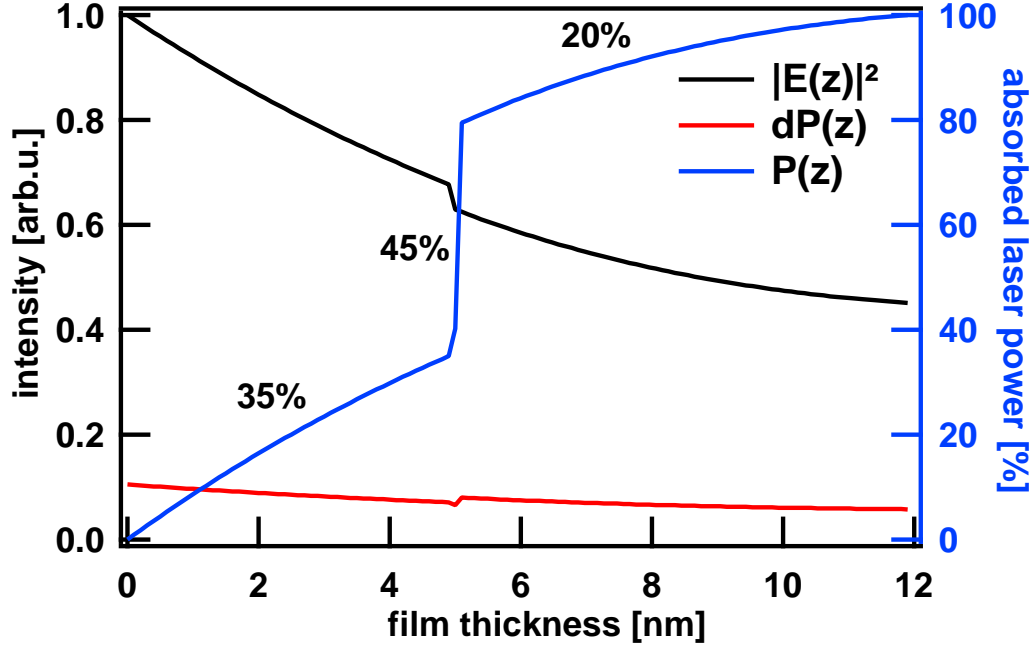


Figure 28: Laser absorption profile for the 200 nm probe beam hitting the surface of 5 nm Au / 7 nm Fe. With the black trace as the intensity of the electric field of the light, the blue the absorbed laser power $P(z)$ normalised to 1 at the end of the sample and the red trace showing the differential of the absorbed laser power $dP(z)/dz$. The first 5 nm are the Au film.

These calculations show where the electrons get excited, besides it should be considered that the electrons need to have enough energy to be above the vacuum level E_{vac} , about 4.9 – 5.1 eV depending on the surface condition, and be close to the Au/vacuum interface to escape the metal and make it into the detector. If all the contributions are summed up the estimated probing depth extends to about 5 – 7 nm into the sample. To calculate the injection efficiency, the fluence of the 1.55 eV pump beam was measured right before entering the vacuum chamber. The incident power was measured with a photodiode power sensor. Eq. 12 shows the relation of the measured power to the fluence on the sample.

$$F = \frac{P [J/s] * \tau_{pulse} [s]}{d_{laser spot} [cm^2]} * c_{loss} [\%] \quad (12)$$

The fluence F is calculated by taking the measured power and multiplying it with the

pulse duration τ_{pulse} and dividing by the laser spot diameter d , that was determined on the CCD camera. Because the pump beam is reflected off one more mirror and gets transmitted through the viewport into the ultra high vacuum chamber a loss of 10% gets added on top. Five of the six experiments were conducted using a fluence of $F = 70 \mu\text{J}/\text{cm}^2$. For the 5 nm Au FP experiment the fluence was increased to $F = 100 \mu\text{J}/\text{cm}^2$ via reducing the optical attenuation, because $F = 70 \mu\text{J}/\text{cm}^2$ was not enough to find a signal.

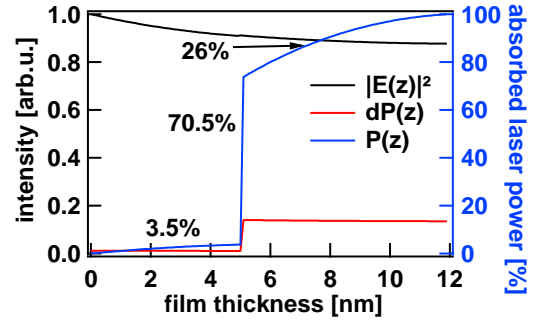


Figure 29: Laser absorption profile for the 800 nm pump beam on the surface of 5 nm Au / 7 nm Fe / MgO in front side pump configuration. The first 5 nm are the Au film.

Combining the incident fluence with the calculated laser beam profiles allows us to calculate the absorbed fluence in the different constituents of the heterostructure. Fig. 29 shows, that not the whole E-field of the laser beam is attenuated, but some of it is transmitted, as indicated by the black line. The incident fluence was multiplied by the absorbed amount, derived from calculation, and then split into the different constituents.

Table 4: Absorbed fluence of the 1.55 eV for the different constituents, all values are given in $\mu\text{J}/\text{cm}^2$

	Au-layer thickness	front side pump		back side pump	
		Fe	Au	Fe	Au
	5 nm	11.87	0.43	12.51	0.175
	15 nm	40.27	2.57	34.2	1.43
	30 nm	62.97	3.32	54.35	3.47

Table 4 shows the different fluences F absorbed in the separate constituents. Unsurprisingly the absorption rises with increasing film thickness, even in Fe layer, which is staying the same size. The more surprising fact is, that the calculations show that even in FP most of the laser power is absorbed inside the Fe-layer. For back side pumping it is assumed, that the observed signal in the p-e TOF is absorbed fluence from the Fe-layer, since the absorption in Au is negligible. The goal here is to compare the different experiments by normalising them among each other.

It was tried to compare the incident fluence with the leaving fluence arriving at the detector.